Photoluminescence study of single ZnO nanostructures: Size effect

L. Feng, C. Cheng, B. D. Yao, N. Wang, and M. M. T. Loy[a)]
Department of Physics, The Hong Kong University of Science and Technology, Hong Kong

(Received 11 June 2009; accepted 17 July 2009; published online 6 August 2009)

Spatially resolved photoluminescence (PL) investigations were carried out on ZnO single nanowires, tetrapods, and nanocrystals. The fractional intensity for bound exciton (BX) transitions was shown to be correlated with the size in all these ZnO nanostructures. This size dependency is attributed to the inhomogeneous density distribution of the defects as binding sites for BX in the ZnO nanostructures, in good agreement with a simple model calculation. © *2009 American Institute of Physics*. [DOI: 10.1063/1.3200232]

ZnO is of great interest for photonic applications due to its direct wide bandgap (3.37 eV at room temperature) and large exciton binding energy (60 meV).[1,2] Fine structures of the near band edge UV peak can be resolved at low temperatures from recombinations of free excitons (FXs), FX phonon replicas, bound excitons (BXs), and donor-acceptor pairs.[3,4] It is well accepted that generally, above 200 K, the dominant peak is due to the transition corresponding to the one-phonon replica of free exciton (FX-1 LO), while at low temperature (<20 K), the dominant peak is that due to BX. While the dominance of the BX peak at low temperature appears to be universal for all ZnO samples, there are still a number of unsolved issues such as the nature of the defects as binding sites for BXs,[5] in particular, whether these are bulk or surface binding sites. In principle, this can be easily settled by measuring the fractional BX photoluminescence (PL) intensity for difference sizes of crystals. A size-dependent fractional BX intensity will point to the importance of surface effects following the change in surface to volume ratio. It is of course essential to ensure that this dependence is actually due to size and not any other factor.[6] In this letter, we report such an experiment using a near field scanning microscopy (NSOM) to perform spatially resolved photoluminescence measurements on single ZnO nanowires, tetrapods, and nanocrystals. The fractional BX PL intensity was shown unambiguously to depend on the size and geometry of ZnO nanostructures in the size range of our study, from ~0.1 to 2 μm, showing inhomogeneous density distribution of binding sites for BXs, in excellent agreement with a simple model given below.

ZnO nanowires and tetrapods were fabricated by thermal evaporation of pure Zn powder without using any catalyst and were dispersed onto a silicon wafer by skimming it over the as-grown sample ensemble.[7] The ZnO nanocrystals were purchased from Nacalai Tesque Inc. and extracting individual ones was achieved by sonication of the ensemble in an ethanol bath and subsequent dropping the solution onto a silicon wafer. The sample morphologies were examined by scanning electron microscopy (SEM) (JEOL6700F). Spatially resolved PL measurements were performed using NSOM (Cryoview2000, Nanonics Inc.) with the excitation at 325 nm from a He–Cd laser via a tapered optical fiber which has a 300 nm aperture. The spatial resolution is about 1 μm and the luminescence was detected by a spectrometer (QE65000, Ocean Optics Inc.) with a spectral resolution of 0.8 nm or ~7 meV at 380 nm.

Three peaks were observed from all the samples at 3.360, 3.308, and 3.235 eV both at 20 and 90 K. We attribute these peaks to be BX, FX-1 LO, and FX-2 LO, respectively,[8–12] although for each of them there may be some minor contributions from other origins. At 20 K, the 3.360 eV (BX) peak is always dominant for all these ZnO nanostructures. The fractional BX intensity B_F, defined as the ratio of BX line to the sum total of the three lines above, is close to unity. At increasing temperatures, B_F decreases monotonically and vanishes at or below 200 K, as shown in Fig. 1(a), when the thermal energy k_BT is equal to the binding energy (~17 meV.) The PL spectrum is then dominated by the FX-1 LO peak. Due to the efficient exciton-phonon coupling in the highly polar material ZnO,[13] the FX line is much smaller and is buried under the "BX" line. This fact conveniently allows us to obtain B_F to a good approximation even though the BX and FX lines were not resolved.

We now discuss the *size dependence* of B_F. For these measurements, the temperature was kept at 90 K. Figure 1

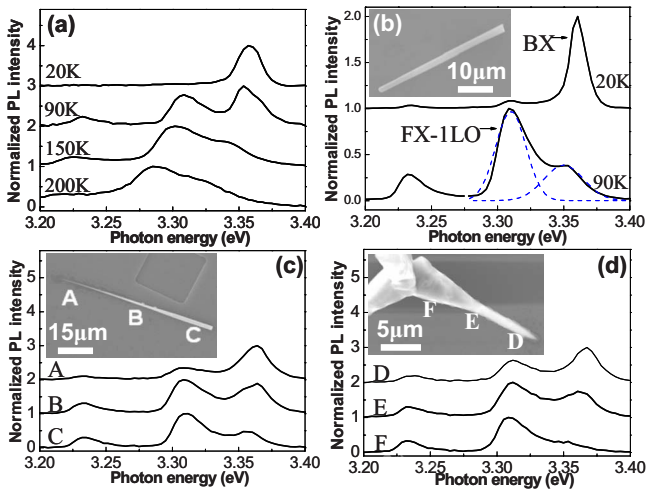

FIG. 1. (Color online) (a) Temperature-dependent PL spectra from position A of a tapered ZnO nanowire (NW a). (b) Normalized PL spectra at 20 K (upper line) and 90 K (lower line) for another ZnO nanowire with the radius of 1.7 μm and the inset is its SEM image. (c) Normalized PL spectra at 90 K both from three positions of the tapered NW a (d) a tetrapod. The insets are their SEM images.

[a)]Author to whom correspondence should be addressed. Electronic mail: phloy@ust.hk.

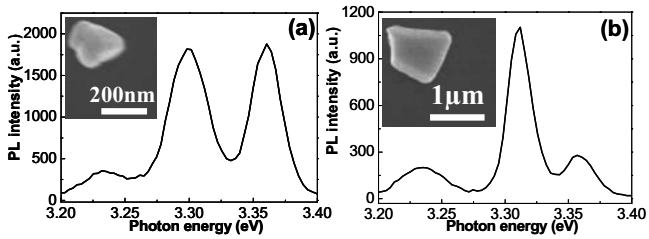

FIG. 2. PL spectra at 90 K from (a) a ZnO nanocrystal whose size is about 200 nm and the inset is its SEM image; (b) a ZnO nanocrystal whose size is about 1.2 μm and the inset is its SEM image.

shows the results from a variety of ZnO nanostructures: tapered nanowires and tetrapods. The electron micrographs show that these structures have varying sizes, ranging from radii of about 100 nm to 2 μm. Using the NSOM, any parts of these nanostructures can be selectively excited with a spatial resolution of better than $(1\ \mu\text{m})^2$. Thus, to a high degree of confidence, any variation in these spatially resolved PL spectra can be attributed to the size of the part of the nanostructures selectively excited. Our results are shown in Fig. 1, and the fractional BX intensity B_F obtained for these sizes are shown in Fig. 3: B_F changes monotonically from ~0.7 for radius of 100 nm, to less than 0.2 for a radius of 2 μm. It is important to note that these B_F values were from different parts of diverse nanostructures as nanowires and tetrapods, yet all follow this unmistakable common dependence on size. As shown below, this dependence can easily be accounted for using a simple model.

The above clearly demonstrates that this size effect does not depend on the specific topography or shape, but only on the size, of our samples. A natural question arises: is this size dependence somehow linked to the particular growth conditions of these nanostructures which, though diverse in shapes, are nonetheless grown under similar conditions? To address this question, we look for ZnO nanostructures that are different in shape from our samples, and not fabricated by us. We use nanocrystals from a commercial source (Nacalai Tesque Inc.). Three such nanocrystals were selected which ranged in size from ~100 to ~600 nm in average radii. The PL results for two of these nanocrystals are shown in Fig. 2 and the resultant B_F shown in Fig. 3. While the values of B_F for these nanocrystals are uniformly smaller than that from the nanowires of similar radii, the same trend

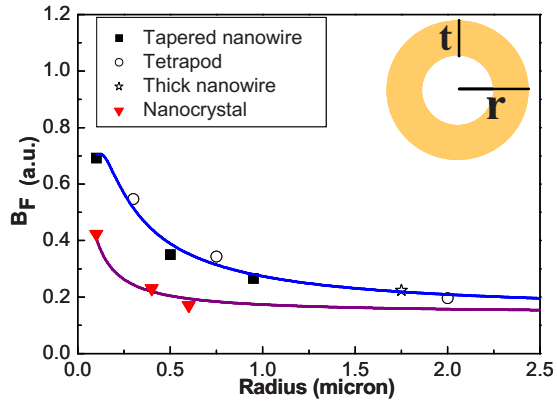

FIG. 3. (Color online) Experimental (points) and fitted data (solid lines) for B_F for nanowires (including tetrapods) and nanocrystals. The inset is a schematic drawing of the cross section of a nanowire. The probability of forming BXs is larger in the darker area.

is clearly seen. B_F varied from ~0.4 at $r=100$ nm to less than 0.17 at $r=600$ nm. This clearly shows that the size dependence of B_F is not only for the ZnO nanostructures fabricated by us, but more likely to be true in general. Needless to say, this effect is observable only with *spatially resolved PL on single nanostructures*; the effect will be averaged out otherwise.

Physically, it appears that the dependence of B_F on size must originate from the changing surface to volume ratio which can be significant in the size range of our study. We propose the following simple model to test this hypothesis on a more quantitative basis, and to see whether the same framework can account for all the data above—both for our nanowires (including tetrapods) and for the commercial nanocrystals using the same set of parameters. Let us assume that there is a layer, with thickness t with an enhanced probability $p+\Delta p$ of forming BXs, the probability being p elsewhere away from the surface,[14,15] schematically shown in Fig. 3, with r as the radius. The *total* number of excitons (electron-hole pairs) is proportional to the volume excited by the incoming UV light, and the number of BXs is the total multiplied by the spatially varying probability as defined above in the model. Thus, for nanowires (and tetrapods) approximated by cylindrical geometry, with a pump beam diameter L smaller than the length of the nanowire, the pumped volume is $\pi r^2 L$ and thus

$$B_F = \frac{N_{\text{BX}}}{N_{\text{exciton}}} = \frac{(p+\Delta p)(\pi r^2 L) - \Delta p[\pi (r-t)^2 L]}{\pi r^2 L}$$
$$= (p+\Delta p) - \frac{\Delta p (r-t)^2}{r^2}. \quad (1)$$

For the nanocrystals, for simplicity, we will approximate using spherical geometry. In this case, the pumped volume is the volume of the sphere, and it is easy to show that for that geometry

$$B_F = (p+\Delta p) - \frac{\Delta p (r-t)^3}{r^3}. \quad (2)$$

We further put some physically reasonable constraints on the parameters to put the cylindrical nanowires and the spherical nanocrystals within the same framework. Far away from the surface, we should expect the probability of forming BX to be independent of size and shape, and so we constrain both nanowires and nanocrystals to have the same p. We further limit the parameter space by choosing Δp to be the same for the two cases as well. With these constraints, it is seen from Fig. 3 that the model prediction is in excellent agreement with all the data with the following values: $p=0.14$, $\Delta p=0.56$; for cylindrical nanowires $t=120$ nm; and for spherical nanocrystals, $t=20$ nm.

Given the simplicity of this model, with the idealized, stepwise probability distribution, the agreement with the experiment is surprisingly good. The model apparently captures the important underlying physics that *there must be a spatially varying distribution of binding sites, and that this is true for all the ZnO nanostructures tested.* In reality, the probability distribution probably varies continuously from surface toward the center. We have also taken the hexagonal cross section of the ZnO nanowire as circular, and taken the

irregular shaped nanocrystals to be spherical, and in both cases the parameters t and Δp are assumed to be independent of crystalline orientation. These parameters, t and Δp, being related to the surface, could in fact depend on surface crystalline orientation. The rather large difference (six times) in t between the cylindrical case and the spherical case should be taken in this light; we have (arbitrarily) constrained Δp to be the same which leads to the large difference in t. However, it is likely that both Δp and t will vary, and might even vary depending on crystalline orientations, and together produce the observed difference in B_F. Given that all our cylindrical samples (nanowires and tetrapods) share the common feature that the growth direction, i.e., the axis of the cylinder is along the [0001] direction, while for the nanocrystals, the surface orientations are likely to be random, different Δp and t for different surface orientations *could* contribute to the observed difference in B_F. To determine whether this hypothesis is correct will require further work. Also, further work will be required to see whether this conclusion and the model will be true for thinner ZnO nanowires below 100 nm. These thinner ZnO nanowires are generally formed in different experimental conditions and their properties are sensitive to many factors, e.g., impurity, absorption, and defects, which must be kept constant. One possible route is to grow tapered nanowires down to tens of nanometers and perform spatially resolved PL as we have done for thicker wires. The model may need modifications as appropriate.

This work is supported by the Research Grants Council of the HKSAR, China (Contract Nos. 602305 and Cityu5/CRF/08).

[1]P. D. Yang, H. Yan, S. Mao, R. Russo, J. Johnson, R. Saykally, N. Morris, J. Pham, R. He, and H. J. Choi, Adv. Funct. Mater. **12**, 323 (2002).
[2]W. Y. Liang and A. D. Yoffe, Phys. Rev. Lett. **20**, 59 (1968).
[3]B. K. Meyer, H. Alves, D. M. Hofmann, W. Kriegseis, D. Forster, F. Bertram, J. Christen, A. Hoffmann, M. Straßburg, M. Dworzak, U. Haboeck, and A. V. Rodina, Phys. Status Solidi B **241**, 231 (2004).
[4]A. Teke, Ü. Özgür, S. Doğan, X. Gu, H. Morkoç, B. Nemeth, J. Nause, and H. O. Everitt, Phys. Rev. B **70**, 195207 (2004).
[5]S. F. J. Cox, E. A. Davis, S. P. Cottrell, P. J. C. King, J. S. Lord, J. M. Gil, H. V. Alberto, R. C. Vilao, J. Piroto Duarte, N. Ayres de Campos, A. Weidinger, R. L. Lichti, and S. J. C. Irvine, Phys. Rev. Lett. **86**, 2601 (2001).
[6]C. Ton-That, M. Foley, and M. R. Phillips, Nanotechnology **19**, 415606 (2008).
[7]L. Feng, C. Cheng, M. Lei, N. Wang, and M. M. T. Loy, Nanotechnology **19**, 405702 (2008).
[8]D. W. Hamby, A. A. Lucca, M. J. Klopfstein, and G. Cantwell, J. Appl. Phys. **93**, 3214 (2003).
[9]D. C. Oh, T. Kato, H. Goto, S. H. Park, T. Hanada, T. Yao, and J. J. Kim, Appl. Phys. Lett. **93**, 241907 (2008).
[10]L. Ding, Ph.D. thesis, The Hong Kong University of Science and Technology, 2007.
[11]Ü. Özgür, Y. I. Alivov, C. Liu, A. Teke, M. A. Reshchikov, S. Doğan, V. Avrutin, S. J. Cho, and H. Morko, J. Appl. Phys. **98**, 041301 (2005).
[12]L. J. Wang and N. C. Giles, J. Appl. Phys. **94**, 973 (2003).
[13]C. Lingshirn, *Semiconductor Optics*, 2nd ed. (Springer, Berlin, 2005).
[14]A. B. Djurišić and Y. H. Leung, Small **2**, 944 (2006).
[15]W. Göpel and U. Lampe, Phys. Rev. B **22**, 6447 (1980).